Journal of Alloys and Compounds 509 (2011) 7585–7590

Contents lists available at ScienceDirect

Journal of Alloys and Compounds

journal homepage: www.elsevier.com/locate/jallcom

Structure and magnetic properties of Cd doped copper ferrite

Radheshyam Rai[a,*], Kavita Verma[b], Seema Sharma[b], Swapna S. Nair[c], Manuel Almeida Valente[c], Andrei L. Kholkin[a], Nikolai A. Sobolev[c]

[a] Department of Ceramics and Glass Engineering and CICECO, University of Aveiro, 3810-193 Aveiro, Portugal
[b] Ferroelectrics Research Laboratory, Department of Physics, A.N. College, Boring Road, Patna 800013, India
[c] Departamento de Fisica, I3N, Universidade de Aveiro, Campus Universitario de Santiago, 3810-193 Aveiro, Portugal

ARTICLE INFO

Article history:
Received 16 December 2010
Received in revised form 6 April 2011
Accepted 6 April 2011
Available online 15 April 2011

Keywords:
Magnetic materials
Chemical synthesis
X-ray diffraction
Magnetic properties

ABSTRACT

This report presents the synthesis of copper cadmium ferrite ($Cu_{1-x}Cd_xFe_2O_4$, $x = 0.3, 0.4, 0.5, 0.6$ and 0.7) by citrate precursor method and its subsequent characterization by using X-ray diffraction (XRD), electron diffraction spectroscopy (EDS) and vibrating sample magnetometer (VSM) techniques. XRD results confirm the single cubic spinel phase formation with the particle size of 40 nm, which decreased up to 20 nm with increases in Cd content, while the lattice parameter increased with increase in Cd content. By using VSM technique, a significant change in the magnetic properties was observed in $CuFe_2O_4$ system with Cd doping. It is seen that magnetic field H_C and remnant magnetization M_R increases with increasing concentration up to $x = 0.6$ except for $x = 0.4$ and 0.7.

1. Introduction

Transition metal oxides (MFe_2O_4) are magnetic materials with cubic spinel structure which are extensively used in various technological applications in the past decades. Dispersions of such magnetic nanoparticles are popularly known as ferro fluids and their emulsions are easy to manipulate with external magnetic field and hence they are extensively used for various fundamental studies [1–4] and technological applications such as optical devices [5], coolants [6,7] sensors [8,9] in biomedical applications, e.g. magnetically guided drug delivery, magnetic resonance image (MRI) contrast agent and cancer therapy [10,11]. Indeed, owing to their high electrical resistivity (over on million times that of equivalent magnetic alloys) that implies low loss due to parasitic currents, and to their susceptibility, they are preferred in application ranging from transformers to magnetic heads. In addition, their high permeability in the r–f frequency region makes polycrystalline ferrites suitable for an increasing number of electron devices [12]. Cubic spinel ferrites crystallizing with space group Fd3m, have been the subject of many recent investigations due to cation distribution. The diversity in properties of ferrites has paved the way for the development of a wide variety of ferrites for various applications such as permanent magnets and electrical and electronic compounds [13,14]. Copper ferrite is an inverse ferromagnetic spinel in which a small amount of Cu^{2+} ions migrate from octahedral B to tetrahedral A sites. The degree of inversion $(Cu_\delta Fe_{1-\delta})^A[Cu_{1-\delta}Fe_{1+\delta}]^BO_4$ (where δ is the inversion parameter and $\delta = 0$ and 1 stand for the inverse and normal cases, respectively), i.e. the fraction of cupric ions at B-sites strongly depends on the preparation technology and temperature which determines the crystal structure [15,16]. Incorporation of zinc and cadmium

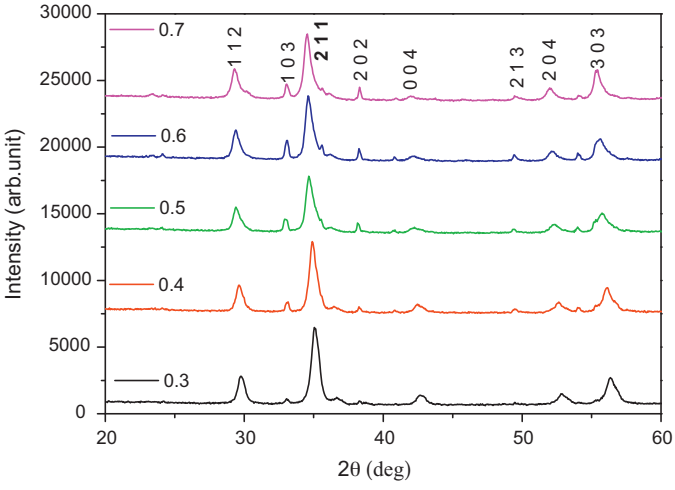

Fig. 1. X-ray diffraction pattern of $Cu_{1-x}Cd_xFe_2O_4$ nanoparticles.

* Corresponding author Tel.: +351 962782932; fax: +351 234425300.
E-mail address: radheshyamrai@ua.pt (R. Rai).

0925-8388/$ – see front matter © 2011 Elsevier B.V. All rights reserved.
doi:10.1016/j.jallcom.2011.04.045

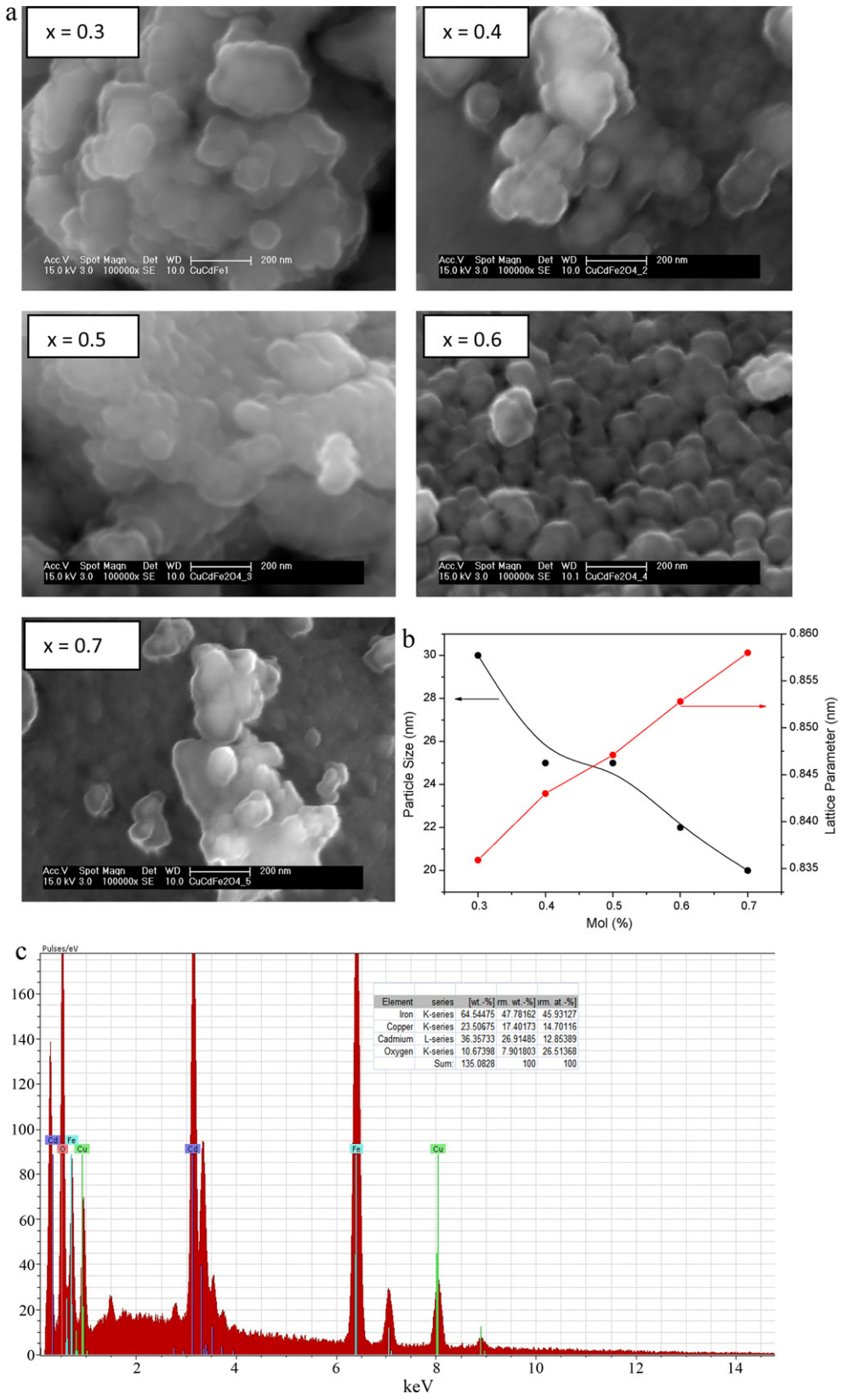

Fig. 2. (a) SEM micrographs of powder specimen of different $Cu_{1-x}Cd_xFe_2O_4$ compositions. (b) Variation of average particle size and lattice parameter with cadmium content. (c) EDX spectrograph of $Cu_{0.5}Cd_{0.5}Fe_2O_4$ composition.

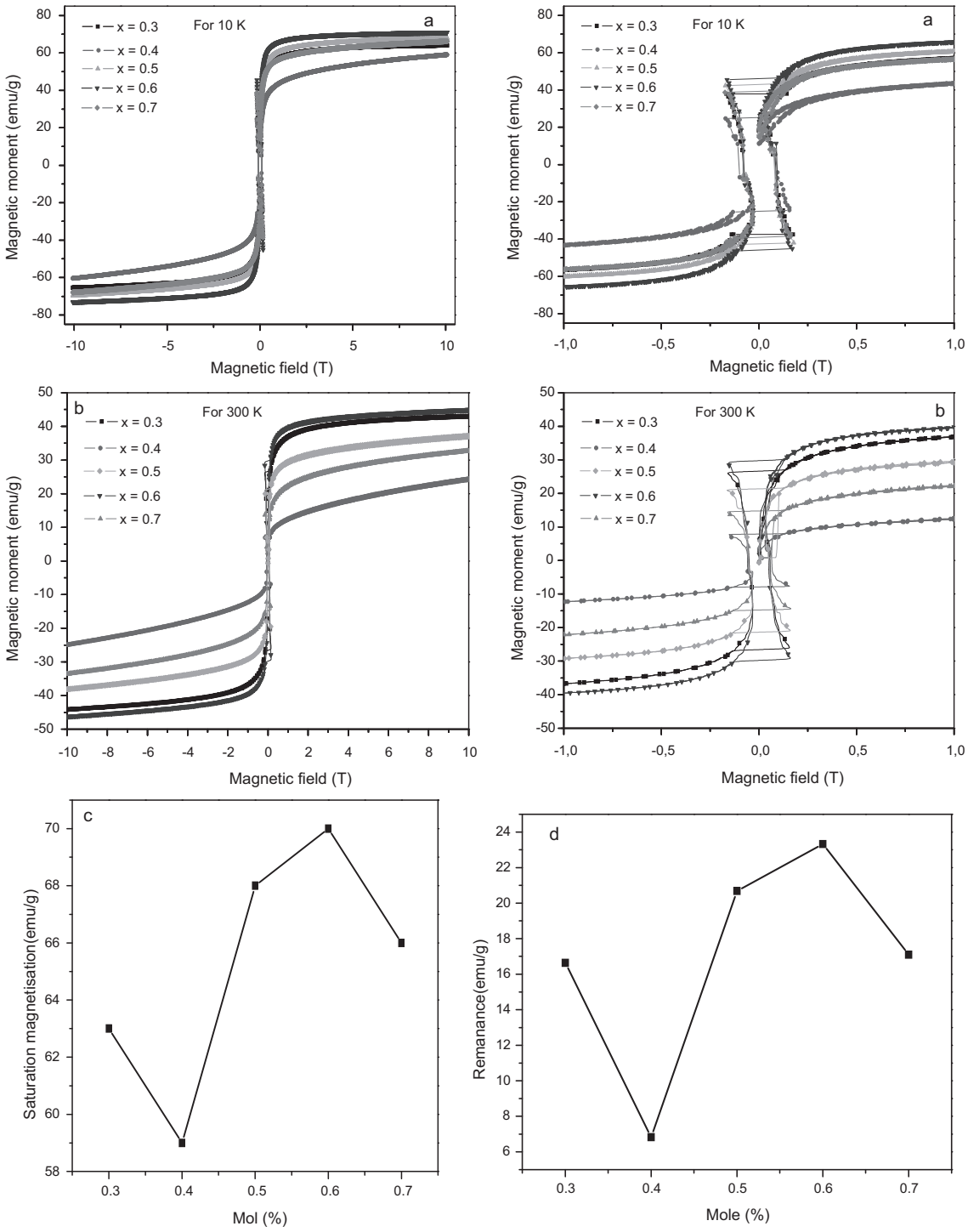

Fig. 3. (a) and (b) M–H loops of $Cu_{1-x}Cd_xFe_2O_4$ at 10 and 300 K. (c) and (d) Saturation magnetization and Remanance vs. composition for $Cu_{1-x}Cd_xFe_2O_4$ at 5 K.

ions strongly affects the magnetic properties of ferrospinel [17] due to its well known preferences for tetrahedral surroundings. It has been reported that cadmium substituted Cu ferrites behaves as n-type semiconductors and the Seebeck coefficient gradually decreases with increase in cadmium content [18]. The composition dependence of some physical parameters such as the density, lattice parameters, porosity, percentage shrinkage, electrical resistivity and thermo electric power of $Cu_{1-x}Cd_xFe_2O_4$ ferrospinel ($0 \le x \le 1$) were studied by Yang et al. [19]. AC electrical parameters such as the dielectric constant (ε_r) and the loss tangent ($\tan\delta$) for slow-cooled and air quenched samples of $Cu_{1-x}Cd_xFe_2O_4$ system (where x varies from 0 to 1) at 400, 600 and 800 °C have been studied as a function of frequency. The cation distribution in $Cu_{1-x}Cd_xFe_2O_4$ ($0.2 \le x \le 1.0$) ferrite system, estimated using X-ray diffraction technique supports the cation distribution predicted by the magnetization method [20]. The physical and chemical properties of these materials can be tuned by controlling the particle size, shape and the inter-particle interactions [21–24].

Due to the vast application of this system, in the present investigation we have prepared nano structured $Cu_{1-x}Cd_xFe_2O_4$ (where x = 0.3, 0.4, 0.5, 0.6 and 0.7) system through thermal decomposition of mixed metal citrates. We attempt to determine the effect of

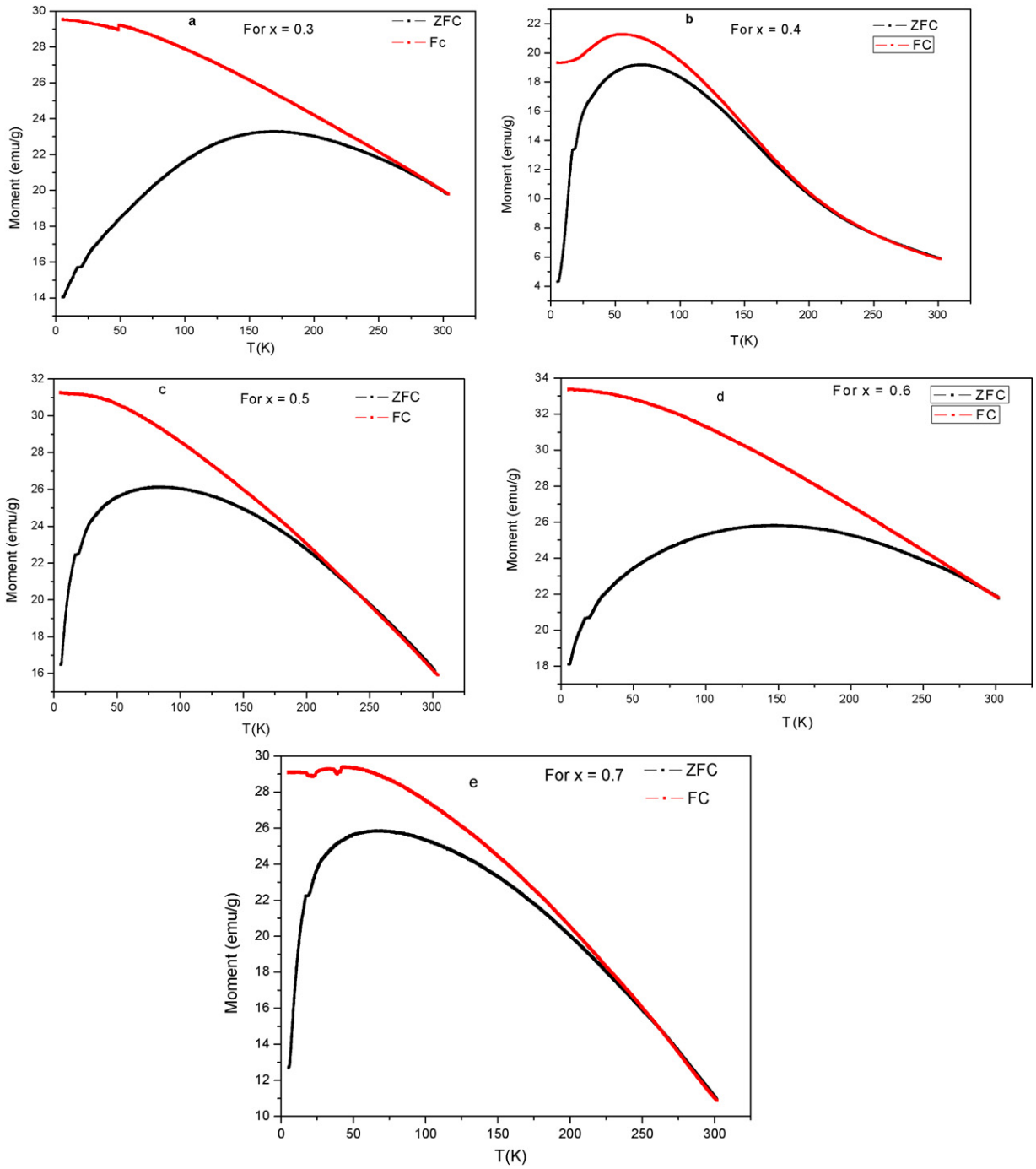

Fig. 4. (a)–(e) The temperature-dependent FC and ZFC magnetization of $Cu_{1-x}Cd_xFe_2O_4$ nano powders.

copper ferrite spinel formation and the role of cadmium content on structural and magnetic properties of these ferrospinels.

2. Experimental procedures

Polycrystalline samples of $Cu_{1-x}Cd_xFe_2O_4$ ceramics with $x = 0.3, 0.4, 0.5, 0.6$ and 0.7 were prepared by citrate precursor method. The technological advantage of this method is the mixing of the metal ions on an atomic scale in the solution state during the initial stages of preparation giving rise to homogeneous mixtures. The chemical precursors used in the preparation were copper nitrate, cadmium nitrate, iron (III) nitrate and citric acid. The chemicals were accurately weighed according to the required stoichiometric proportion. An aqueous solution of Fe(III) citrate was prepared in distilled water. Copper nitrate and cadmium nitrate was separately mixed with citric acid and few drops of distilled water and heated at about 40 °C for an hour to form the metal-citrate complex. These solutions were then added slowly to the Fe(III) citrate solution with constant stirring to avoid precipitation. A homogeneous solution of brown-colored citrate mixture was obtained with no precipitation and no segregation of phases. This mixture was gradually heated at 60 °C on a hot plate with a magnetic stirrer to obtain slurry. The precursor was obtained by drying it in the oven. This solid precursor was in the form of a uniformly colored brown transparent glassy material containing the cations homogeneously mixed on an atomic scale. This dried citrate mixture was calcined in muffle furnace for 4 h at 600 °C to obtain a spinel ferrite of the compound $Cu_{1-x}Cd_xFe_2O_4$. The calcined compounds were grounded in a mortar pestle to obtain fine powder. The fine powders were used to characterize the structural and micro structural properties of the compound. The X-ray diffraction pattern of the compounds was recorded at room temperature using X-ray powder diffractometer with CuK_α radiation ($\lambda = 1.5418$ Å) in a wide range of Bragg angles 2θ ($20^\circ \leq 2\theta \leq 60^\circ$) at a scanning rate of 2° min^{-1}. SEM micrographs of the powder specimens were acquired with the help of a JEM-2000FX (JEOL Ltd.) scanning electron microscope (operated at 20 keV). Magnetic characterization was carried out using a vibrating sample magnetometer (VSM) (Cryogenic) with an applied magnetic field up to 1 T.

3. Results and discussion

The X-ray diffractograms of $CuCdFe_2O_4$ ferrite system (Fig. 1) reveal the single-phase spinel structure without any ambiguous reflection. The experimentally observed d spacing values and relative intensities are in well agreement with those reported in the ASTM powder diffraction files. The calcined powder samples show XRD peaks at d = 2.97, 2.59, 2.50, 2.06 and 1.59 Å and they are in good agreement with the standard XRD pattern, JCPDS (34-0425) of $CuFe_2O_4$. The lattice parameters are obtained by fitting at least seven diffraction peaks using standard least square refinement methods. The lattice parameters are in the expected range with the lattice constant of $CuFe_2O_4$ [25] and $CdFe_2O_4$ [26] at either end. Lattice parameter increases linearly with the increase of cadmium content. This could be attributed, as expected, to the large ionic radius of Cd^{2+} (0.78 Å) which when substituted in the lattice resides on the tetrahedral site and replaces the smaller Cu^{2+} (0.57 Å) or Fe^{3+} (0.49 Å) ions from the tetrahedral to the octahedral site [20]. No other phase is observed in XRD graph indicating that no chemical transformation took place during the heat treatment. This XRD graph indicated that the synthesized powders contain nanosized crystallites.Fig. 2(a) illustrates the results of scanning electron microscopic observation of the $Cu_{1-x}Cd_xFe_2O_4$ nanoparticles. The segregation of impurity is not observed. The variation of average particle size with Cd content is shown in Fig. 2(b). The average particle size decreases with Cd content, which is attributed to the diffusion phenomenon involving Cd, oxygen vacancies and porosity that hampers the grain growth. The SEM micrograph shows that the particle size is about 20–40 nm. This value is in accordance with that obtained from XRD measurements. It can be seen that these samples also show spherical morphology with uniform diameter of about 20 nm. By adjusting some growth parameters, such as reaction time and temperature, the initial concentration, the size of these $Cu_{1-x}Cd_xFe_2O_4$ microspheres is controllable to be 20–30 nm in diameters [27–29]. Energy dispersive X-ray analysis (EDAX) was also used to determine the chemical composition of the as-prepared ferrite products. Results from EDAX spectra from individual as-prepared ferrite microspheres showed that samples only contain Cd, Cu, Fe, and O for $CuFe_2O_4$ Fig. 2(c).

In general, copper ferrites are inverse spinel ferromagnetic materials. However, the degree of inversion is deeply related to the synthesis techniques adopted. However, just like zinc, cadmium has strong tetrahedral preference which makes the A–B interactions affect the net magnetic moment in AB_2O_4 ferrites. However, a higher magnetic moment can be achieved if the cadmium ions can move to the octahedral sites. In order to probe into these effects, copper ions were substituted with cadmium ions. Magnetic hysteresis loops were traced for all the samples at 10 K and 300 K in a field range of 0–1 T and are shown in Fig. 3(a) and (b). It is seen that magnetization and remanence curves follow exactly the same pattern against the cadmium substitution in copper ferrites with x = 0.6 showing the highest value for M_S and M_R (Fig. 3(c) and (d)). This can be explained as follows. The magnetic properties of ferrite materials depend on the particle size, sintering temperature, additives, micro structure, applied external field and also due to the partial inversion of copper ferrite which could give the possibility of getting both the copper and cadmium ions occupying the tetrahedral sites making the A–A interactions also accountable. The effect of concentration (x) on magnetic properties is clearly perceptible in the evolution of hysteresis loop indicating that Cd doped $CuFe_2O_4$ has introduced ferromagnetic contribution. Jiang et al. [30] has also reported that in $CuFe_2O_4$ ceramics, a weak ferromagnetism is introduced which was attributed to the continuing collapse of space-modulated spin structure in these samples. The origin of improved magnetic properties may be traced to increased canting effect by a structural distortion or uncompensated anti-parallel sub-lattice magnetization on A site doping [31]. However, in our system, a high saturation magnetization is observed which is close to that observed for ferro/ferromagnetic samples. Hence in this system, the canting of spins makes them no more antiferromagnetic. The unusual ferromagnetic like heavy saturation magnetization is indicative of a ferrimagnetic ordering induced by the cation redistribution which is common in ferrites synthesized by wet chemicals methods like co-precipitation, sol–gel, citrate precursor methods, etc.

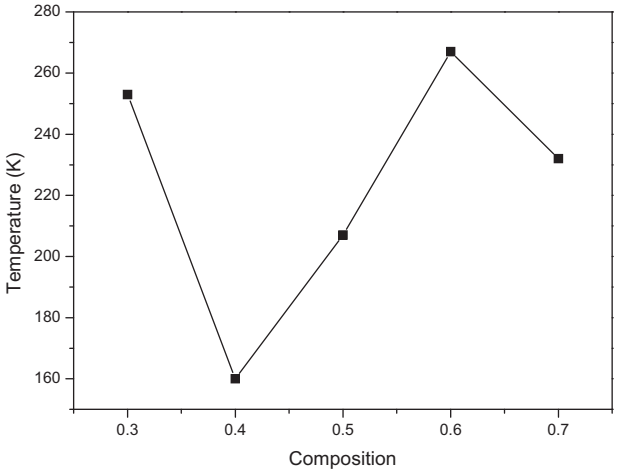

Fig. 5. Variation of magnetic transition temperature with x.

The expanded low field regimes of the hysteresis loops (Fig. 3(a) and (b)) show a magnetic switching behavior for all the samples which makes them ideal for switching applications in which magnetization suddenly drops to almost negligible values at a specific applied field.

In order to probe in to the nature of magnetic transition, and to measure the transition temperature the magnetization vs. temperature (Fig. 4(a)–(e)) was measured in the field cooled (FC) as well as zero field cooled (ZFC) mode. The transition temperature can be defined as the temperature at which the ZFC and FC curves bifurcate. The plot of transition temperature vs. the composition is shown in (Fig. 5). In order to probe into the magnetic transitions happening in the samples, the M–T measurements were carried out in FC and ZFC modes. It shows that the transition temperature is shifted due to the Cd substitution and the ZFC and FC bifurcates well before the peak in ZFC. The transition is very broad in samples with x = 0.3 and 0.6 while the transition is more sharp for the other samples. The transition is much broader than spin glass systems and the difference in ZFC and FC value at 10 K is much higher so that it cannot be accounted for the spin canting effect.

The FC curves of systems of independent single-domain particles are expected to exhibit a monotonic increase below the temperature of the maximum in ZFC, T_{max}. In systems of particles with moderate interactions, these can dominate over the privileged direction set by the external field, thus causing the FC curve to remain at a constant value below T_{max}. However in strongly interacting magnetic systems like spin glass, the FC decreases below the temperature in which the ZFC peaks. In our case, for the samples with x = 0.3 and 0.7, the FC decreases after the ZFC peak showing strong interactions between the particles, while in all the other systems, FC shows an increase below the ZFC peak showing independent single domain like particles. However, an exact type of transition can be confirmed only with a field dependent ZFC–FC studies or ac susceptibility studies [32–34].

4. Conclusions

In this report, cadmium doped copper ferrite has been synthesized by citrate precursor method, with a ferrite spinel structure. The particle size of copper ferrite was 40 nm, which decreased to 20 nm with increase in Cd concentration. SEM micrographs show spherical morphology with uniform particle distribution. All the samples exhibited ferromagnetic nature at room temperature with appreciable value of remanent magnetization. Switching of magnetic moments from a higher value to zero is observed for all the samples at a specific applied magnetic field.

References

[1] Q.A. Pankhurst, A.J. Pollard, J. Phys. Condens. Matter 5 (1993) 8487.
[2] Q.A. Pnakhurst, J. Connolly, S.K. Jones, J. Dobson, J. Phys. D 36 (2003) R167.
[3] J. Philip, G. Gnanaprakash, T. Jayakumar, P.K. Sundaram, B. Raj, Macromol. Surf. Colloid. Interact. 36 (2003) 9230.
[4] I.I.S. Lim, P.N. Njoki, H.Y. Park, X. Wang, L. Wang, D. Mott, C.J. Zhong, Nanotechnology 19 (2008) 305102.
[5] A.R. Lamani, H.S. Jayanna, P. Parameswara, R. Somashekar, Ramachander, R. Rao, G.D. Prasanna, J. Alloys Compd. 509 (2011) 5692–5695.
[6] J. Philip, P.D. Shima, B. Raj, J. Appl. Phys. 91 (2007) 203108.
[7] J. Philip, P.D. Shima, B. Raj, J. Appl. Phys. 92 (2008) 043108.
[8] M. Pitaa, J.M. Abad, C. Vaz-Dominguez, C. Briones, E. Mateo-Martí, J.A. Martín Gago, M. del, P. Morales, V.M. Fernandez, J. Colloid Interface Sci. 321 (2008) 484.
[9] J. Philip, T. Jaykumar, P.K. Sundaram, B. Raj, Meas. Sci. Technol. 14 (2003) 1289.
[10] P. Tartaj, P.M.del. Morales, S. Veintemillas-Verdaguer, T. Gonzalez-Carreno, C.J. Serna, J. Phys. D 36 (2003) R182.
[11] L. Kaufner, R. Cartier, R. Wustneck, I. Fichtner, S. Pietschmann, H. Bruhn, D. Schutt, A.F. Thunemann, U. Pison, Nanotechnology 18 (2007) 115710.
[12] A. Goldman, Modern Ferrites Technology, Marcel Decker, NY, 1993.
[13] A. Meenakshisundaram, N. Gunasekaran, V. Srinivasan, Phys. Status. Solidi A 69 (1982) k15.
[14] B.V. Bhise, A.K. Ghatage, B.M. Kulkarni, S.D. Lotke, S.A. Patil, Bull. Mater. Sci. 19 (3) (1996) 527.
[15] A. Pradeep, P. Priyadharsini, G. Chandrasekaran, J. Alloys Compd. 509 (2011) 3917–3923.
[16] E. Prince, R.G. Srivastava, N.G. Navadikar, Phys. Rev. B 14 (1976) 2032.
[17] C.M. Srivastava, S.N. Shringi, R.G. Sristava, N.G. Navadikar, Phys. Rev. B 14 (1975) 2032.
[18] L. Suber, R. Zysler, A. García Santiago, D. Fiorani, M. Angiolini, A. Montone, J.L. Dormann, Mater. Sci. Forum 937 (1998) 269–272.
[19] Z.H. Yang, Z.W. Li, L. Liu, L.B. Kong, J. Alloys Compd. 509 (2011) 3038–3041.
[20] B.P. Ladgaokar, A.S. Vaingankar, Mater. Chem. Phys. 56 (1998) 280.
[21] C. Burda, X. Chen, R. Narayanan, M.A. El-Sayed, Chem. Rev. 105 (2005) 1025.
[22] A.G. Roca, M.P. Morales, K. O'Grady, C.J. Serna, Nanotechnology 17 (2006) 2783.
[23] X. Teng, H. Yang, Nanotechnology 16 (2005) S554.
[24] X. Cao, L. Gu, Nanotechnology 16 (2005) 180.
[25] A.A. Choni, A.I. Etyhhand, A.A. Mohamed, Proc. Int. Conf. Ferrites, 5, 1980, p. 216.
[26] M. UL-Islam, T. Abbas, M.A. Chaudhry, Mater. Lett. 53 (2002) 30.
[27] H. Deng, H. Chen, H. Li, Mater. Chem. Phys. 101 (2007) 509–513.
[28] G. Viau, R. Brayner, L. Poul, N. Chakroune, E. Lacaze, F.F. Vincent, F. Fi'evet, Chem. Mater. 15 (2003) 486–494.
[29] B. Wiley, T. Herricks, Y. Sun, Y. Xia, Polyol. Nano Lett. 4 (2004) 1733–1793.
[30] J.Z. Jiang, G.F. Goya, H.R. Rechenberg, J. Phys. Condens. Matter 11 (1999) 4063–4078.
[31] S. Si, C. Li, X. Wang, D. Yu., Q. Peng, Y. Li, Cryst. Growth Des. 5 (2005) 391.
[32] Z.H. Zhou, J.M. Xue, J. Wang, H.S.O. Chan, T. Yu, Z.X. Shen, J. Appl. Phys. 91 (2002) 6015.
[33] R.A. Borzi, S.J. Stewart, G. PPunte, R.C. Mercader, G. Cernicchiaro, F. Garcia, Hyperfine Interact. 148 (2003) 109.
[34] G. Catalan, J.F. Scott, Adv. Mater. 21 (2009) 2463.